

## Supplemental Materials

### Multi-stage explosion of lignin: A new horizon for constructing defect-rich carbon towards advanced lithium ion storage

Caiwei Wang<sup>a</sup>, Dongjie Yang<sup>a,\*</sup>, Si Huang<sup>a</sup>, Yanlin Qin<sup>b,c</sup>, Wenli Zhang<sup>b,c</sup> and Xueqing Qiu<sup>b,c,\*</sup>

<sup>a</sup> School of Chemistry and Chemical Engineering, Guangdong Provincial Engineering Research Center for Green Fine Chemicals, South China University of Technology, Guangzhou 510640, China

<sup>b</sup> School of Chemical Engineering and Light Industry, Guangdong University of Technology, Guangzhou, 510006, China

<sup>c</sup> Guangdong Provincial Key Laboratory of Plant Resources Biorefinery, 100 Waihuan Xi Road, Panyu District, Guangzhou 510006, China

**\*Corresponding Authors:** Prof. Dongjie Yang, Xueqing Qiu

**E-mail address:** [cedjyang@scut.edu.cn](mailto:cedjyang@scut.edu.cn) (D. Yang), [cexqqiu@scut.edu.cn](mailto:cexqqiu@scut.edu.cn) (X. Qiu).

#### Table of Contents

Supplementary Figures.....	1
Supplementary Tables.....	7
References.....	8

## Supplementary Figures

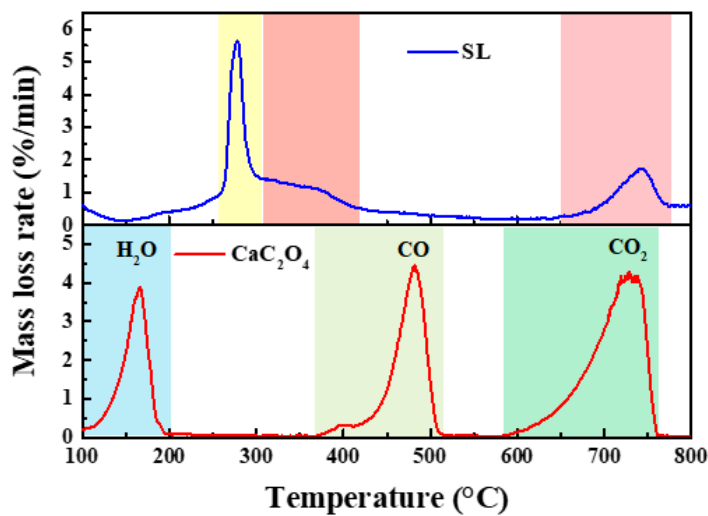


**Fig. S1.** DTG curves of SL and CaC<sub>2</sub>O<sub>4</sub>.

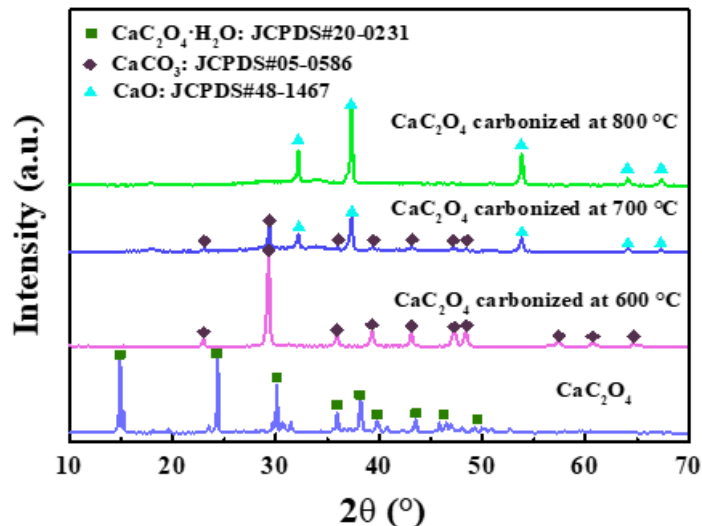


**Fig. S2.** XRD patterns of CaC<sub>2</sub>O<sub>4</sub> carbonized at 600-800 °C. The diffraction peak of pure CaC<sub>2</sub>O<sub>4</sub> fits well with that of CaC<sub>2</sub>O<sub>4</sub>·H<sub>2</sub>O (JCPDS #20-0231). The diffraction peak of CaC<sub>2</sub>O<sub>4</sub> carbonized at 600 °C accords well with those of CaCO<sub>3</sub> (JCPDS #05-0586), indicating that CaC<sub>2</sub>O<sub>4</sub> was completely decomposed into CaCO<sub>3</sub> at 600 °C. CaC<sub>2</sub>O<sub>4</sub> carbonized at 700 °C presents the diffraction peak in good agreement with CaCO<sub>3</sub> (JCPDS #05-0586) and CaO (JCPDS #48-1467), indicating that CaCO<sub>3</sub> was partially decomposed into CaO at 700 °C. The diffraction peak of CaC<sub>2</sub>O<sub>4</sub> carbonized at 800 °C coincides with those of CaO (JCPDS 48-1467), indicating CaCO<sub>3</sub> was completely decomposed into CaO at 800 °C.

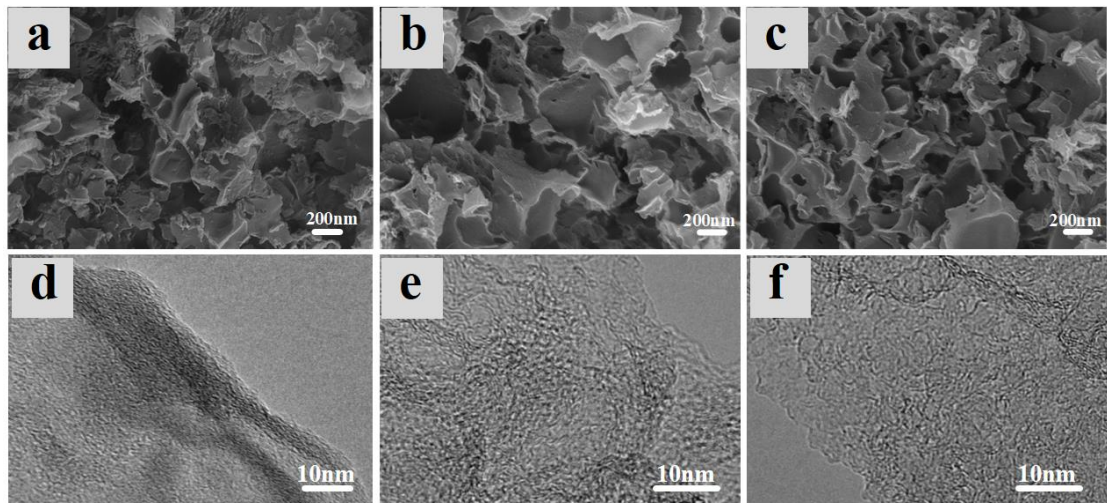


**Fig. S3.** SEM images of (a) PLPCC-600, (b) PLPCC-700, (c) PLPCC-800. HRTEM images of (d) PLPCC-600, (e) PLPCC-700, (f) PLPCC-800.

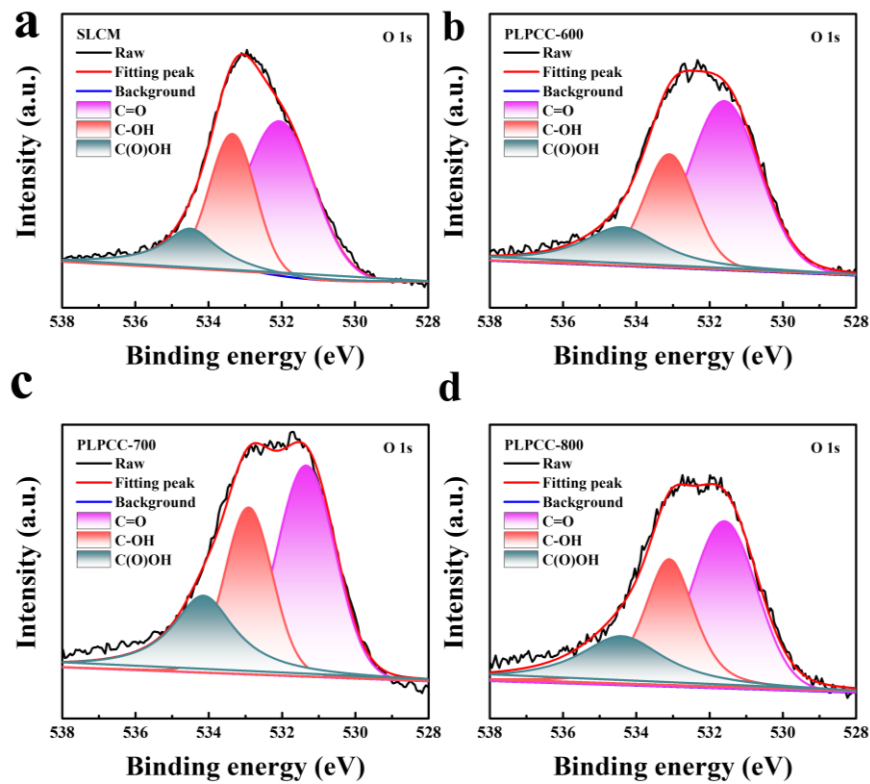


**Fig. S4.** Deconvolution of high-resolution O 1s spectra of PLPCCs and SLCM.

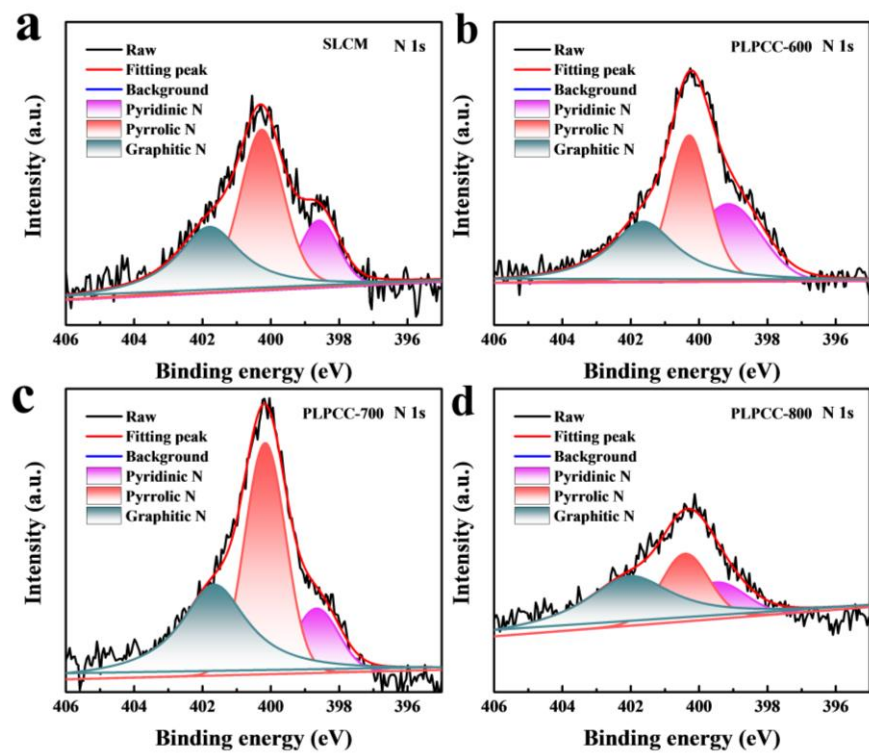


**Fig. S5.** Deconvolution of high-resolution N 1s spectra of PLPCCs and SLCM.

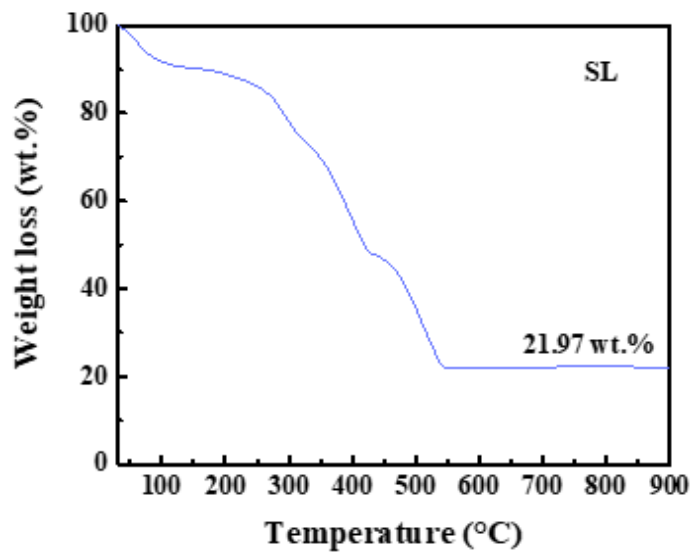


**Fig. S6.** TG curves of SL under air atmosphere. After air heat treatment at 900 °C, the ash residue of SL is 21.97 wt.%.

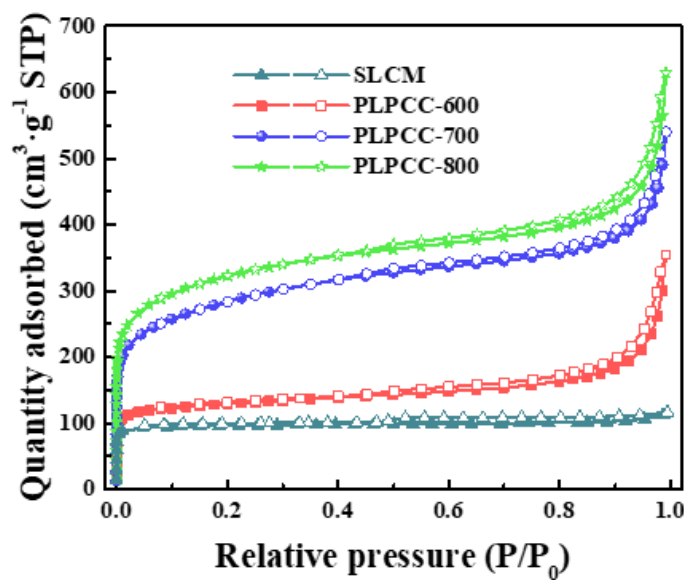


**Fig. S7.** Nitrogen adsorption and desorption isotherms.

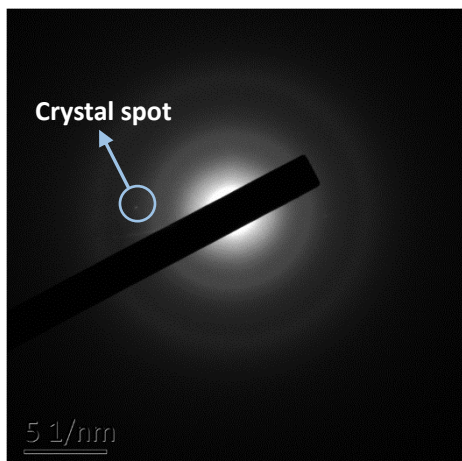


**Fig. S8.** SEAD pattern of PLPCC-700.

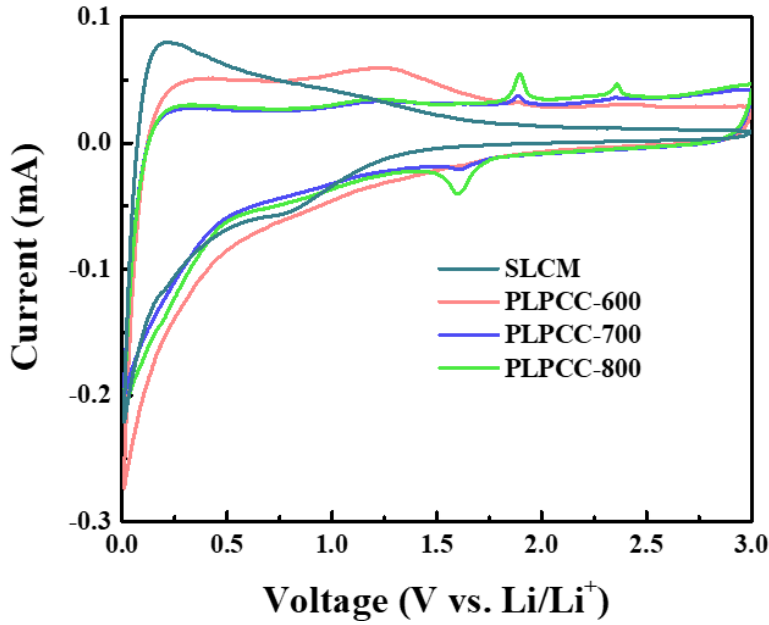


**Fig. S9.** The first CV curves of electrodes.

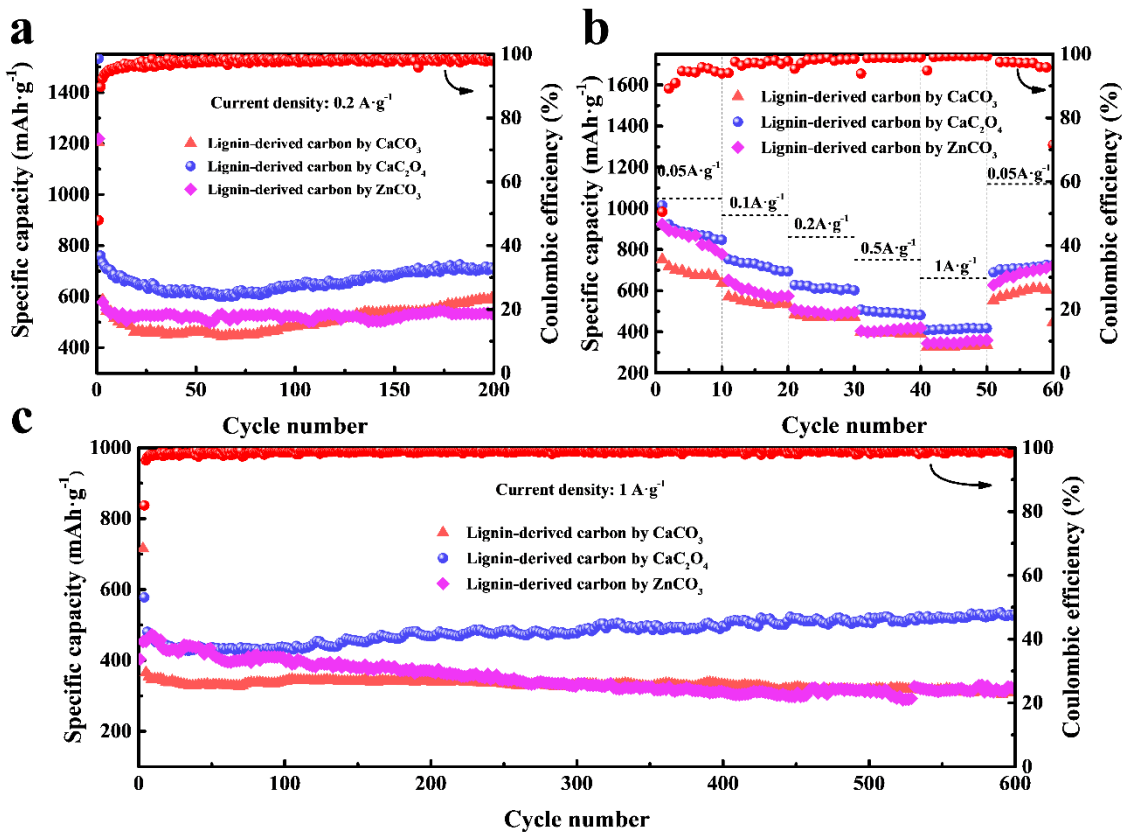


**Fig. S10.** Comparison of lithium storage capabilities of the lignin-derived carbons prepared by  $\text{CaCO}_3$ ,  $\text{CaC}_2\text{O}_4$  and  $\text{ZnCO}_3$ . (a) GCD curves at  $0.2 \text{ A}\cdot\text{g}^{-1}$ . (b) Rate performance at  $0.05\text{--}1 \text{ A}\cdot\text{g}^{-1}$ . (c) Long-cycling performance at  $1 \text{ A}\cdot\text{g}^{-1}$ .

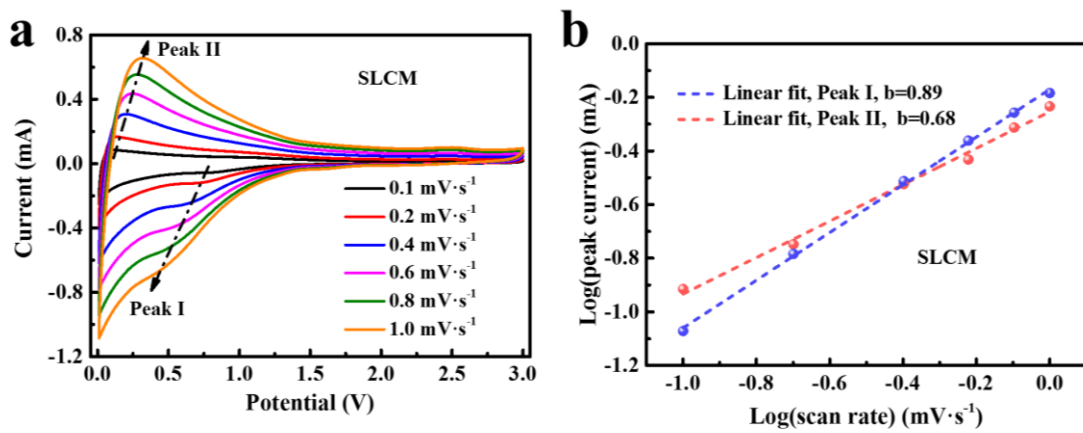


**Fig. S11.** (a) CV curves of SLCM at different scan rates. (b) Determination of *b* values.

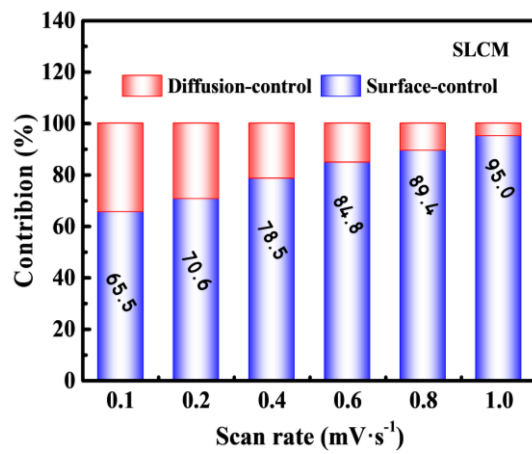


**Fig. S12.** (a) Capacitance-controlled and diffusion-controlled contribution of SLCM.

## Supplementary Tables

**Table S1** Surface O and N configurations of SLCM and PLPCCs.

Samples	Percentage of <i>O</i> -containing groups			Percentage of <i>N</i> -containing groups		
	C=O	C-OH	COOH	N-6	N-5	N-Q
SLCM	28.2	47.2	24.6	15.9	46.2	37.9
PLPCC-600	53.3	27.3	19.4	24.5	37.0	38.5
PLPCC-700	52.3	25.0	22.7	13.2	43.9	42.8
PLPCC-800	43.2	31.5	25.3	17.7	27.6	54.7

**Table S2** Textural properties of SLCM and the PLPCC samples at 600-800°C.

Samples	$S_{\text{BET}}$ (m <sup>2</sup> /g)	$V_{\text{total}}$ (cm <sup>3</sup> /g)	$V_{\text{mic}}$ (cm <sup>3</sup> /g)	$V_{\text{meso}}$ (cm <sup>3</sup> /g)	$V_{\text{mic}}/V_{\text{total}}$ (%)	$V_{\text{meso}}/V_{\text{total}}$ (%)	$D_{\text{avg}}$ (nm)
SLCM	385.5	0.15	0.12	0.02	80.0	13.3	1.87
PLPCC-600	491.3	0.49	0.17	0.23	34.7	46.9	3.01
PLPCC-700	1028.7	0.75	0.35	0.32	46.7	42.7	2.58
PLPCC-800	1175.6	0.87	0.41	0.36	47.1	41.4	2.57

$S_{\text{BET}}$ : Specific surface area was determined using the Brunauer-Emmett-Teller (BET) equation.

$V_{\text{total}}$ : Total pore volume was determined by NLDFT model.

$V_{\text{mic}}$ : Micropore volume was determined by NLDFT model.

$V_{\text{meso}}$ : Mesopore volume was determined by NLDFT model.

**Table S3** Specific capacities of PLPCCs tested under the current density of 0.2 and 1 A·g<sup>-1</sup>.

Electrodes	Specific capacity (mAh·g <sup>-1</sup> )			
	0.2 A·g <sup>-1</sup>		1 A·g <sup>-1</sup>	
	25th	200th	100th	600th
SLCM	235.1	256.1	165.0	209.7
PLPCC-600	455.5	543.2	322.9	386.5
PLPCC-700	642.5	706.3	436.9	530.4
PLPCC-800	445.8	618.5	289.3	448.7

**Table S4** Comparison of lithium storage performance of PLPCC-700 with different carbonaceous materials in the reported literatures.

Materials	Specific surface area (m <sup>2</sup> ·g <sup>-1</sup> )	ICE <sup>a</sup> (%)	Cycling data <sup>b</sup>	Rate capacity <sup>c</sup>	Ref.
PLPCC-700	1029	49.2	706/200/200	530/1000	This work
Hierarchical porous carbon (HPC)	420	40.4	390/50/37	266/1860	[1]
Hierarchical porous carbon (LHPC)	907	41.6	470/275/200	268/1000	[2]

Hierarchical porous carbon (HLPC-ZnCO <sub>3</sub> -600)	531	54.9	550/200/200	315/1000	[3]
Hierarchical porous carbon (KHPC-600)	735	47.3	650/60/100	346/5000	[4]
Macroporous carbon (MPC-3)	631	54.3	501/120/200	306/1000	[5]
Nanoporous hard carbon microspheres (NHCS-6)	753	45.0	230/30/100	157/1490	[6]
Carbon nanofibers/nanosheets hybrid (CNFS)	847	-	592/200/100	508/1000	[7]
Graphene aerogels (GA)	530	-	439/30/100	250/1000	[8]
N-doped carbon nitride (CNNC)	-	-	430/60/50	323/2500	[9]

<sup>a</sup> Initial coulombic efficiency

<sup>b</sup> Capacity (mAh·g<sup>-1</sup>)/cycle numbers/current density (mA·g<sup>-1</sup>)

<sup>c</sup> Capacity (mAh·g<sup>-1</sup>)/current density (mA·g<sup>-1</sup>).

## References

- [1] J. Yang, X. Y. Zhou, Y. L. Zou and J. J. Tang, *Electrochim Acta*, 2011, **56**, 8576-8581.
- [2] W. L. Zhang, J. Yin, Z. Q. Lin, H. B. Lin, H. Y. Lu, Y. Wang and W. M. Huang, *Electrochim Acta*, 2015, **176**, 1136-1142.
- [3] Y. B. Xi, S. Huang, D. J. Yang, X. Q. Qiu, H. J. Su, C. H. Yi and Q. Li, *Green Chem*, 2020, **22**, 4321-4330.
- [4] D. P. Qiu, C. H. Kang, M. Li, J. Y. Wei, Z. W. Hou, F. Wang and R. Yang, *Carbon*, 2020, **162**, 595-603.
- [5] Y. X. Fu, X. Y. Pei, D. C. Mo and S. S. Lyu, *J Mater Sci-Mater El*, 2019, **30**, 5092-5097.
- [6] S. M. Jafari, M. Khosravi and M. Mollazadeh, *Electrochim Acta*, 2016, **203**, 9-20.
- [7] S. B. Wang, C. L. Xiao, Y. L. Xing, H. Z. Xu and S. C. Zhang, *J Mater Chem A*, 2015, **3**, 6742-6746.
- [8] Y. X. Xu, Z. Y. Lin, X. Zhong, B. Papandrea, Y. Huang and X. F. Duan, *Angew Chem Int Edit*, 2015, **54**, 5345-5350.
- [9] W. L. Zhang, J. Yin, C. L. Chen and X. Q. Qiu, *Chem Eng Sci*, 2021, **241**, 116709.